

ACCOUNTS of CHEMICAL RESEARCH[®]

APRIL 2000

Registered in U.S. Patent and Trademark Office; Copyright 2000 by the American Chemical Society

Molecular Tennis—Flat Smashes and Wicked Cuts

ANDREW J. ALEXANDER AND
RICHARD N. ZARE*

*Chemistry Department, Stanford University,
Stanford, California 94305-5080*

Received October 18, 1999

ABSTRACT

Molecular photodissociation typically produces open-shell photofragments that have angular momentum. This Account explores how the measurement of the directional nature of photofragment angular momentum can provide us with a new viewpoint for seeing and understanding the process whereby molecules fall apart under irradiation. Although the photodissociation process is more complicated than might be imagined at first, the measurements reveal detail that approaches conventional bound-state spectroscopy, enhancing our understanding of the chemical bond and even allowing us to manipulate the ultimate fate of a photofragment by selecting the wavelength and the polarization of the photolysis source.

1. Birth of a Chemical Bond

Much of our understanding of the chemical bond has grown from experiments using spectroscopy, that is, the interaction between light and matter.^{1,2} Measurements of specific energies and intensities of light absorbed by a molecule yield detailed clues about the structure and dynamics (motion) of the nuclei. Quite simply, a molecule consists of a framework of atomic nuclei that are held together by electrons from each atom; the negatively

charged electrons conspire to have charge density at the right places to offset the repulsion of the positively charged nuclei. Thus, the chemical bond is really a matter of electrostatics, the balancing of electrical forces that arise from Coulomb's law. The problem, of course, is to know where the electrons are so that the equilibrium structure, corresponding to the balance configuration, can be calculated.

Consider the case of a simple diatomic molecule: in general, the atoms that come together to make a chemical bond are electronically open-shell; there are one or more unfilled orbitals with principal quantum number n . An atom has the symmetry of a sphere, and the open-shell electrons may possess a net electronic angular momentum, comprising of orbital angular momentum (quantum number L) and spin angular momentum (quantum number S). What happens when we bring together two atoms? Clearly we are changing the symmetry of our system. We start with two spherical objects, and we finish with a molecule that has an axis of cylindrical symmetry, that is, the bond axis. This new symmetry dictates that we can no longer use the quantum numbers of our separated spherical atoms. Instead, we must describe the quantization of angular momenta as (signed) projections on the new symmetry axis, making orbital and spin quantum numbers Λ and Σ . The sum of these two projections, in which Λ is always given a positive sign, is denoted by Ω .¹ Molecular states that have the same values of Λ but different values of Ω have different energies. The energy splittings are relatively small compared to the separation between different electronic states; they arise from magnetic effects, such as spin-orbit coupling. The so-called Wigner-Witmer rules give us a recipe for enumerating the types and numbers of different molecular electronic states of definite symmetry that arise from combining the individual atomic angular momenta.^{3,4} How we relate Ω to the orbital (L) and spin (S) quantum numbers depends on the type of coupling between the different angular momenta. When the electric field gradients between the nuclei are high, especially at small internuclear separations, L and S may couple separately to the internuclear axis, making projections Λ and Σ respectively, with total

Andrew J. Alexander was born in Elgin, Scotland (1972), was educated at Edinburgh University (B.Sc. 1994) and Oxford University (D.Phil. 1997), and is presently a postdoctoral research associate in the Zare group. His scientific interests focus on studies of elementary chemical reactions.

Richard N. Zare was born in Cleveland, OH (1939), was educated at Harvard University (B.A. 1961, Ph.D. 1964), and is currently the Marguerite Blake Wilbur Professor in Natural Science at Stanford University. His scientific interests encompass a wide range of disciplines, ranging from laser studies of chemical processes to development of new tools for analytical chemistry of biological systems.

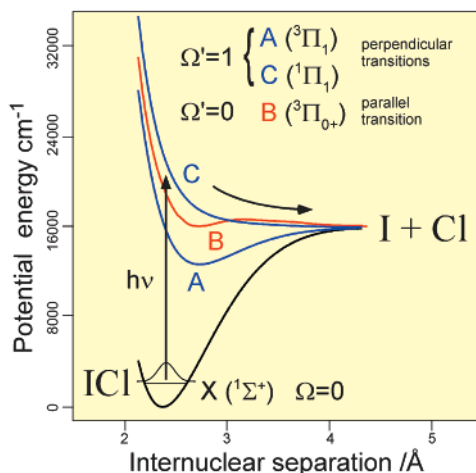


FIGURE 1. Schematic figure showing potential energy as a function of internuclear separation for the ICl molecule. Each curve shown in the figure represents a different electronic state. Absorption of a photon from the ground electronic state (X) is represented as a vertical arrow (with energy $h\nu$) at the so-called Franck–Condon region of internuclear separation. Molecules may then dissociate on any of the three surfaces (A, B, or C) to give I and Cl atoms.

projection Ω —this is referred to as Hund’s case (a) coupling.¹ When the electric field gradients are weak, at larger internuclear separation, the spin and orbital angular momenta couple to each other, but the total projection on the internuclear axis, Ω , remains a good quantum number—we refer to this coupling scheme as Hund’s case (c).¹

As an example, let us consider the simple interhalogen diatomic molecule iodine monochloride (ICl). Each ground-state atom has a 2P term, meaning that $L = 1$ and $S = 1/2$. The possible electronic states are then $\Lambda = 0$ (called a Σ state), $\Lambda = 1$ (called a Π state), and $\Lambda = 2$ (called a Δ state). The electronic spin multiplicity can be $(2\Sigma + 1) = 1$ (singlet) or $(2\Sigma + 1) = 3$ (triplet). In fact, for the ground electronic state of ICl, the electrons pair up to produce $^1\Sigma^+$, where the superscript plus sign simply refers to the symmetry of the electronic wave function, which is unchanged upon reflection in a plane containing the internuclear axis.^{5,6}

Bringing atoms together to make bonds sounds simple in principle, but the details of making or breaking a molecular bond are not straightforward. Indeed, for the most part, an exact solution of the Schrödinger equation for such a problem is prohibitively expensive. We are partly saved by one approximation, the Born–Oppenheimer approximation, which assumes that the time scale for motion of the nuclei is sufficiently slow for the electrons to rearrange at each nuclear configuration.^{7,8} We may map out the potential energy for each configuration of the nuclei to form an adiabatic potential energy surface (PES).⁹ This mapping is illustrated in Figure 1, which shows the four lowest adiabatic PESs for ICl.¹⁰ For adiabatic dissociation in which the nuclei move in the same electronic state, the projection of the total electronic

angular momentum Ω on the internuclear axis is conserved as the molecule dissociates.

In Figure 1, the lowest surface $X(^1\Sigma^+)$ is the ground electronic state of ICl and exhibits a potential minimum. Electronic excitation by a photon with energy $h\nu$ (h is Planck’s constant, and ν is the frequency) is shown schematically as a vertical arrow from the ground state. Note that three of the surfaces have bound-state minima, but the C state does not: it is purely repulsive. Molecules that find themselves on a repulsive PES are destined to fall apart, as indicated by the curved arrow. Surfaces that include a minimum are capable of supporting quantized energy levels, and it is by excitation connecting one quantized level to another quantized level that spectroscopy has produced much detailed information about the structures of *bound* molecules.² Unfortunately, however, details of the *unbound* surfaces or the structure of bound surfaces above their bound limits cannot be obtained so simply. Excitation to a state beyond its dissociation limit typically shows a spectrum with a broad, structureless absorption feature that reveals relatively little about the structure of the surface or the excitation process.¹¹ How can we characterize and learn about such states?

2. Death of a Chemical Bond

Photodissociation of a molecule occurs when the molecule absorbs sufficient radiant energy to become excited above the dissociation threshold.^{7,11} There is no requirement for excitation to a purely repulsive state: even states that contain a bound minimum may contribute to the dissociation, either directly or by transferring population to another state during the dissociation process. Although somewhat of an oversimplification, it is tempting to treat the photodissociation process as two steps: (1) absorption of one (or more) photons to a state above the dissociation threshold, followed by (2) dissociation of the nuclei. Classically, in the excitation step, the electrons are induced to oscillate by the oscillating electric field of the light, and energy is absorbed when the oscillation frequency matches the Bohr condition, $\Delta E = h\nu$, where ΔE is the energy difference between the upper and lower molecular energy levels.⁵ The interaction occurs via an oscillating electric transition dipole in the molecule, and this transition dipole has a well-defined symmetry in terms of the nuclear configuration.⁶ For a simple diatom, like ICl, the transition dipole can be either parallel or perpendicular to the bond. We can take advantage of the polarized nature of light to probe the symmetry of the transition dipole, as illustrated schematically in Figure 2. The linearly polarized light consists of an oscillating electric field that is aligned in space; the double-headed arrow in Figure 2 denotes the direction of the polarization of the oscillating electric field, ϵ . If we dissociate an ensemble of molecules using linearly polarized light in the laboratory, molecules that have their transition dipoles aligned parallel to the electric polarization vector will absorb energy preferentially. The probability for excitation depends on the relative directions of the electric polarization vector (ϵ) and the transition

* Corresponding author. E-mail: zare@Stanford.EDU.

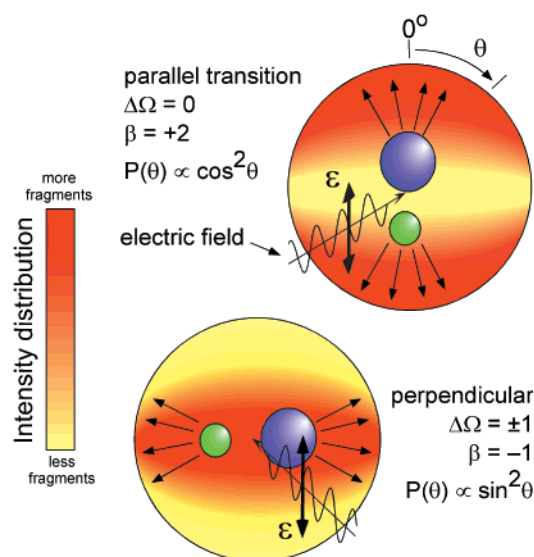


FIGURE 2. Illustration of the absorption of a linearly polarized photon by a diatomic molecule. The two possible types of transition are shown; see text for details. The resulting distribution of fragments is schematically shown, with red indicating the most fragments and yellow indicating no fragments.

dipole moment (μ), $I \propto |\mu \cdot \epsilon|^2$ (i.e., a scalar product of two vectors).¹² Assuming that the fragments instantly recoil, the resulting direction of the product fragments directly reveals the symmetry of the excitation process (see Figure 2). For a parallel transition, the angular distribution of the resulting fragments is $P(\theta) \propto \cos^2 \theta$, and for a perpendicular transition it is $P(\theta) \propto \sin^2 \theta$, where θ is the angle between ϵ and the direction (velocity) of the photofragment. In fact, the angular distribution may be described by

$$P(\theta) = [1 + \beta P_2(\cos \theta)]/4\pi$$

where the parameter β takes the limiting values $+2$ for a $\cos^2 \theta$ (parallel) distribution and -1 for a $\sin^2 \theta$ (perpendicular) distribution, and $P_2(\cos \theta) = (3 \cos^2 \theta - 1)/2$ is the second-order Legendre polynomial.

The symmetry of the transition dipole with respect to the diatomic molecule (parallel or perpendicular to the bond) is directly related to the electronic symmetry of the PES. Parallel transitions excite from $\Omega = 0$ of the ground electronic state to $\Omega' = 0$ of the upper state (e.g., surface B in Figure 1); perpendicular transitions excite from $\Omega = 0$ to $\Omega' = 1$ (e.g., states A and C of Figure 1). By measuring the directions of the product fragments, we may, in many cases, determine which states are involved in the excitation process. In the case of ICl photodissociation using visible light, the transition is almost purely parallel ($\beta \sim +2$) at short wavelengths (490 nm), becomes a mixture of parallel and perpendicular ($\beta \sim 0$) at intermediate wavelengths (ca. 525 nm), and tends toward almost purely perpendicular ($\beta \sim -1$) at longer wavelengths (560 nm).¹³ Unfortunately, however, measurement of the angular distribution of the fragments alone cannot tell us which or how much of the $\Omega' = 1$ states, A or C, is involved in the photodissociation. Likewise, the angular distribution

does not tell us much about the detailed shapes of the PESs traversed en route to the product asymptotes.

3. Anyone for Molecular Tennis?

The measurement of the angular distribution of a photofragment, that is, the direction of the product relative to the electric vector of the light beam, can give us important clues about the symmetry of the electronic surfaces excited in the dissociative absorption process. Measurement of the angular distribution, however, provides only limited information on the dissociation process. Evidence for nonadiabatic transitions between surfaces can rarely be obtained directly, and the angular distributions yield little or no clues about the dynamics of the dissociating molecule that occurs far from the vertical Franck–Condon excitation region. In particular, angular distributions teach us very little about the detailed shapes of the PESs.¹⁴ Another strategy for probing the photodissociation dynamics is to measure the electronic angular momentum of one or both fragments, which can be achieved using polarized light to detect the products by spectroscopy.^{15–17} Because the electrons form the “fabric” of the PES, measurement of product electronic angular momentum directly yields information on the electronic symmetries and shapes of the surfaces followed during photodissociation.^{18–21}

In the case of ICl photodissociation, the Cl atom photofragments can be probed using either left or right circularly polarized light, which is sensitive to the handedness, or orientation, of the electronic angular momentum of the atoms.²² The orientation of the atoms arises from unequal population of their electronic magnetic sublevels, m_J and $-m_J$. In the laboratory frame, through an excited $J = 1/2$ state, we can use *left* circularly polarized light to ionize Cl atoms from the $m_J = -1/2$ and $-3/2$ levels with the spectroscopic selection rule $\Delta m_J = +1$. Conversely, the selection rule for *right* circularly polarized light is $\Delta m_J = -1$, which preferentially ionizes Cl atoms in the $m_J = +1/2$ and $+3/2$ levels. By counting how many ions are produced for each polarization, we determine the relative populations of the $\pm m_J$ sublevels, and therefore the overall orientation of the Cl atom photofragments.²² From a classical viewpoint, the orientation can be associated with atoms that have topspin or backspin with respect to their direction of motion. The orientation of product Cl atoms was measured over a range of photolysis wavelengths from 490 to 560 nm, and the Cl atoms were found to oscillate between topspin and backspin several times over the range of photolysis energies,^{10,13,23} as shown in Figure 3a. How does this orientation arise? The observed orientation is dependent on the simultaneous (coherent) excitation of states of both parallel and perpendicular symmetry. Viewed classically, a parallel transition induces electrons to oscillate along the molecular axis; for a perpendicular transition, the electrons oscillate to and fro perpendicular to the molecular axis. As the molecule dissociates, both of these motions experience different potential energies as they travel over the surfaces on which they were

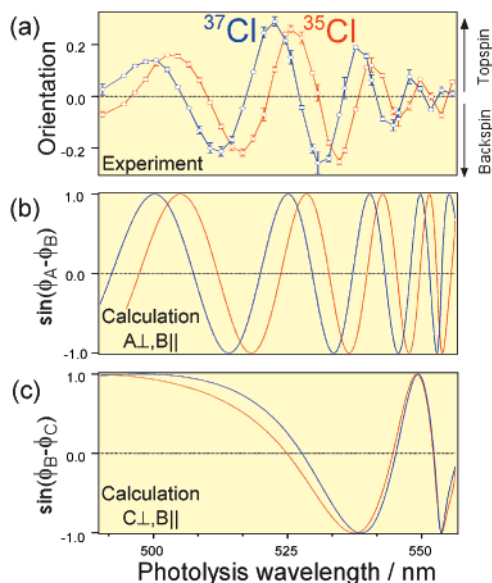


FIGURE 3. Observed orientation of the electronic angular momentum of Cl atoms over a range of photodissociation wavelengths. Results for two isotopes of Cl are shown. (a) Experimental results, showing oscillation between positive and negative orientation (shown as topspin and backspin). (b) Theoretical calculations that show the phase difference between waves on the A and B curves (see Figure 1, and text for more details). (c) Theoretical calculations that show the phase difference on the C and B curves. The experimental results are most closely matched by the calculations shown in (b).

created. The difference in potential energy results in a phase difference between the parallel and perpendicular oscillations of the electrons. The resultant asymptotic phase difference causes the net oscillation to have a circular component (see Figure 4). Quantum mechanically, we may view the mixed transition as having two incoherent terms: a pure parallel transition, a pure perpendicular transition, and a coherent “interference” term that results from the superposition of dissociative states excited by our photolysis radiation.^{19,24}

To understand the importance of the mixed transition, let us draw upon an analogy with two types of shots that can be played in tennis. A parallel transition or a perpendicular transition causes, in tennis parlance, a flat smash of the tennis ball so that it has no preference to spin one way or another. A mixed transition corresponds to a wicked cut, causing the tennis ball to spin with respect to its direction of motion, either with topspin or backspin, as illustrated in Figure 5. Actually, we need to think about both the Cl atom and the I atom: the cut that causes Cl to have topspin also causes I to have topspin, but because the recoil directions of I and Cl are oppositely directed, the two topspins cancel in sum. Indeed, this cancellation is a perfect one in that the entire system—uniformly distributed ICl bond axes and linearly polarized light beam—has no handedness (chirality) before absorbing the photon that causes dissociation. Likewise, the entire system after absorbing a photon of linearly polarized light

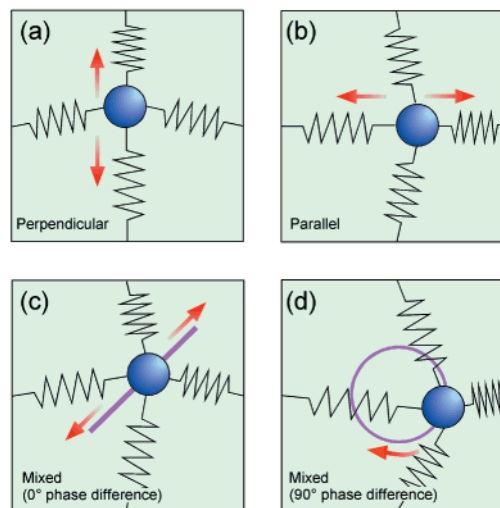


FIGURE 4. Illustration showing how adding a parallel and a perpendicular motion can lead to different types of net motion, including circular. The thought experiment consists of a ball attached by four springs in a square cage. Panel (a) shows a vertical (say, perpendicular) motion, while (b) shows a horizontal (say, parallel) motion. If we combine these two motions, the ball being fully up while being fully to the right, we get a linear motion at 45° (panel c) in the cage: the two motions are in phase. It is also possible to imagine the ball being up, then right, then down, then left, and so on, in which case the up–down motion is happening “in between” the left–right motion. This is a motion that appears circular, as illustrated in (d). Now imagine that the up–down springs are of a different strength from the left–right springs—this will cause a difference in the frequency of the two motions. If we start the ball as in panel (c), it will first move at 45° and then slowly become elliptical and then circular in motion as the phase between the parallel and perpendicular motions changes with time.

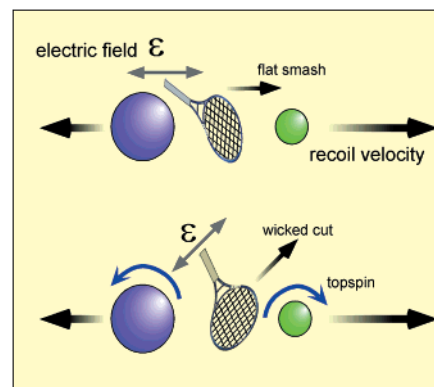


FIGURE 5. Molecular tennis: a purely classical mechanical (i.e., fictional) illustration. The simple diatomic molecule ICl is shown. A pure parallel or perpendicular transition is represented as a flat smash (top figure). The atomic fragments have no topspin or backspin. Putting the racket at an angle (corresponding to a mixture of parallel and perpendicular), we get a so-called wicked cut: the resulting fragments both are topspinning with respect to their direction of travel. See text for a more lucid description of this type of tennis.

must not have any net handedness—it therefore follows that the cancellation is exact.

But why does the orientation oscillate between topspin and backspin over the range of photolysis energies? The asymptotic phase difference introduced between parallel

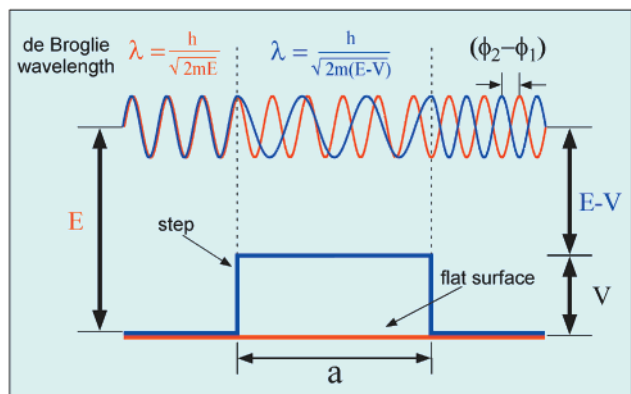


FIGURE 6. Simple quantum mechanical illustration of the asymptotic phase difference between the wave functions associated with fragments that travel over different PESs. The red surface is flat (constant potential energy, $V = 0$). The blue surface has a step of potential energy, height V . Also shown are two de Broglie waves, of energy E . The wavelength of the de Broglie wave depends on E and V , as shown. Look at the figure from left to right. In regions where the waves feel the same potential energy, they have the same wavelength. At the left-hand side they are the same and in phase. The blue wave oscillates more slowly when it flies over the potential step of height V . At the right-hand side the waves have the same wavelength but now a different phase. The phase difference ($\phi_2 - \phi_1$) depends on the height of the step (V), the width (a), and the energy (E).

and perpendicular symmetries is dependent on the shapes of the PESs followed during the dissociation. A simple analogy is obtained by considering a one-dimensional potential step, shown in Figure 6. A particle that experiences a flat potential has a constant de Broglie wavelength. The de Broglie wavelength of a particle above the potential step is longer, such that the final phase difference between the two paths is dependent on the height (V) and width (a) of the step and on the energy of the particle (E) as it approaches the step. Returning to our real-life photodissociation, we excite molecules of parallel and perpendicular symmetry that access surfaces of different potential energy. At the dissociation asymptote, the difference in phase between perpendicular and parallel components of the fragment electronic angular momentum gives a net circular (orientation) component. As we tune the photolysis energy, the sine of the asymptotic phase difference, $\sin(\phi_{\text{perpendicular}} - \phi_{\text{parallel}})$, will change and may oscillate between positive and negative values depending on the potential energies encountered. The oscillation of the sine of the phase difference is the cause of the observed oscillation between topspin and backspin in the case of ICl photolysis.

Another curious observation is the difference in the oscillations for the two naturally occurring isotopes of chlorine: the oscillations for ^{35}Cl and ^{37}Cl are displaced relative to each other, as shown in Figure 3a. The two isotopes of chlorine each experience the same PES as they dissociate, but they have different masses. This mass difference directly manifests itself in different de Broglie wavelengths, which results in a small relative displacement in the phase of the oscillations. Recall that the de Broglie wavelength is $\lambda = h/mv$, where m is mass and v is velocity

of the fragment.⁵ It is worth noting in passing that iodine has only one naturally occurring isotope, ^{127}I .

Simulations of the experimentally measured oscillations allow us to fine-tune model PESs, affording detailed information on the fabric of the molecular bond.¹⁰ The simulations involve solution of the one-dimensional Schrödinger equation using theoretically calculated ab initio PESs: the results of the simulations are shown in Figure 3b,c. As can be seen from the simulations, the oscillating phase difference is quite well reproduced. Also, it is found that only states A and B (see Figure 1) are required to reproduce the observed oscillations; state C apparently contributes very little, if anything, to the transition. The amplitudes of the experimental oscillations are observed to decrease toward either extreme of the photolysis range explored. In fact, the oscillations are multiplied by a factor that depends on the amount of parallel and perpendicular transition involved. At 490 nm the transition is predominantly parallel, and the handedness is very small because we only have a small amount of perpendicular transition. Likewise, at 560 nm, the transition is predominantly perpendicular. At intermediate photolysis wavelengths, around 525 nm, the transition is equally mixed, and the amplitude of the observed oscillation is largest.¹³

In summary, it has been shown that measurement of energy-dependent photofragment orientation provides a probe that is sensitive to the precise shape of the dissociating PES, detail that is on a par with conventional bound-state spectroscopy. Moreover, the measurements of the atomic fragment angular momenta demonstrate that the convenient fiction of drawing the ICl bond as a straight line connecting the I and Cl atoms, I–Cl, should not mislead us into thinking that the actual bond is one-dimensional. Our game of molecular tennis, with its wicked cuts arising from mixed state transitions, shows that the molecular bond really has a complex three-dimensional structure. Of course, this fact was already indirectly known from various other experiments, such as X-ray crystallography, which have given us information on the electron density contours in a molecule.^{5,25} But this game of molecular tennis is more than just about the structure of the chemical bond; as we shall discuss further, it also tells us about the dynamics of the electron charge cloud as the molecule falls apart into its constituent pieces.

4. See How They Run and Jump

Measurement of the energy dependence of the product orientation yields information about the shapes of the dissociating surfaces excited in transitions involving states of different symmetry. So far, we have not considered fragments that cross from one PES to another during dissociation. The validity of the Born–Oppenheimer approximation greatly depends on the speed of recoil of the atoms, the strength of spin–orbit interactions, and the proximity of other nearby electronic states. Deviations from the Born–Oppenheimer approximation involve non-adiabatic interactions and crossings between adiabatic

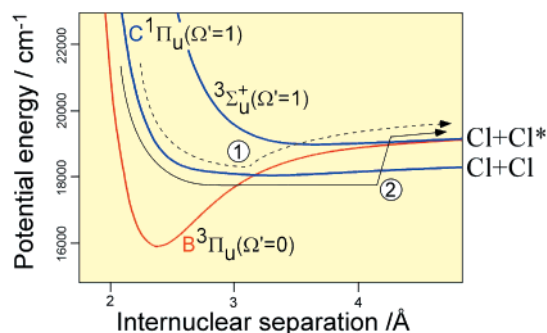


FIGURE 7. Electronic states accessed in the ultraviolet photodissociation of Cl_2 (see text). Unlike Figure 1, the ground electronic state is not shown. Production of excited-state chlorine atoms $\text{Cl}^*(^2\text{P}_{1/2})$ occurs by excitation to, and direct dissociation on, the B state. Cl^* may also be produced by excitation to the C state, followed by a nonadiabatic crossing. Excitation directly to the higher triplet $^3\Pi_u$ ($\Omega' = 1$) state does not occur, as this involves a change in the spin (the ground state is a singlet). Two mechanisms for the nonadiabatic crossing are shown in the figure, labeled (1) and (2), and are described in the text.

surfaces. At short internuclear distances, strong coupling between the different flavors of angular momenta (spin, orbit, or molecular rotation) may induce nonadiabatic transitions between case (a) surfaces. At larger internuclear distances, where the system is best described by case (c) coupling, nonadiabatic transitions may occur by uncoupling of the spin–orbit interaction or by the radial kinetic energy of the system, that is, how fast the bond is broken.^{7,8}

In the near-ultraviolet photodissociation of molecular chlorine (Cl_2) nonadiabatic transitions occur, producing a small percentage of chlorine atoms that are electronically excited, $\text{Cl}^*(^2\text{P}_{1/2})$ along with ground-state $\text{Cl}(^2\text{P}_{3/2})$ atoms.^{26,27} The subscript of the term symbol (^{2S+1}L) tells us the magnitude of the total angular momentum, J . For chlorine atoms, $S = 1/2$ and $L = 1$, and they add vectorially to give $J = |L - S| = 1/2$ or $J = L + S = 3/2$. The two angular momentum states have different energies, with the $J = 3/2$ state being the ground state. The ground electronic state of Cl_2 is $^1\Sigma_g^+$, where the g denotes that the electronic wave function is unchanged with respect to interchange of the two identical Cl nuclei.^{5,6}

In the photodissociation of Cl_2 , excited-state Cl^* atoms can originate either from direct dissociation via a parallel transition to the B state or from perpendicular excitation to the C state, followed by nonadiabatic crossing to surfaces correlating to produce Cl^* atoms. For the particular case of Cl_2 photodissociation, two viable mechanisms exist for the crossing. These mechanisms are illustrated schematically in Figure 7. Crossing directly from the C ($\Omega' = 1$) to the B ($\Omega' = 0$) states may occur (mechanism 1), induced by rotational angular momentum of the Cl_2 molecule. Alternatively, crossing from the C ($\Omega' = 1$) to higher states of $\Omega' = 1$ symmetry may also occur (mechanism 2); these higher states directly correlate to produce Cl^* atoms.²⁸ The latter mechanism is induced by the kinetic energy of the fragments as they “blast” apart: the Born–Oppenheimer approximation breaks down, and the molecule does not know whether it is on surface C or

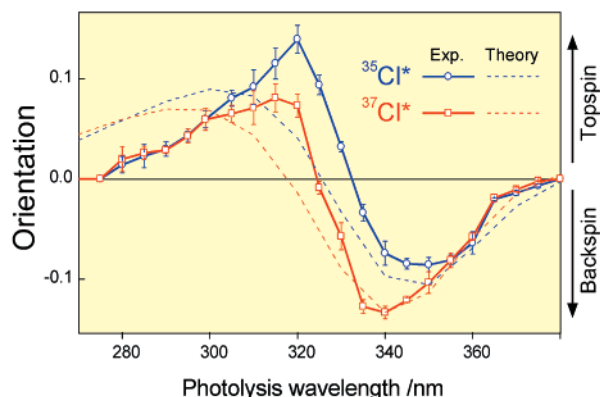


FIGURE 8. Similar to Figure 3, but showing orientation of excited-state Cl^* atoms following photodissociation of Cl_2 over a range of photolysis wavelengths. Experimentally measured Cl^* orientation is shown (points and solid lines), along with calculations (dashed lines). Details are given in the text.

some other surface of the same ($\Omega' = 1$) symmetry (in this mechanism, Ω must be conserved). Figure 8 presents the experimentally determined Cl^* product orientation measured as a function of photodissociation wavelength, showing a single oscillation over the range investigated.²⁹

In the ICl photodissociation described above, several oscillations from topspin to backspin were observed over the range of photolysis energies investigated. So why do we only see only a single oscillation for Cl_2 photodissociation? For Cl_2 photodissociation, the absorption of the ultraviolet photons (ca. 350 nm) brings us much higher in energy above the dissociation threshold than in the case of ICl photolysis (ca. 530 nm). As we tune the photolysis energy, we are less sensitive to the difference between the two PESs encountered, and the sine of the phase difference between the two paths changes sign only once over the energy range accessed. So, why not tune to longer wavelengths, that is, lower photolysis energies? Unfortunately, at longer wavelengths the absorption of Cl_2 becomes prohibitively weak and eventually tails off to zero.²⁷

Figure 8 shows the results of simulations using theoretically predicted ab initio PESs that include kinetic energy coupling (mechanism 2). Theoretical simulations of the data using a rotationally induced spin–orbit coupling (mechanism 1) are not so successful in reproducing the experimental points.²⁹ As can be seen from this figure, experiment and theory are in quite reasonable agreement, which suggests that the kinetic energy coupling mechanism is mostly responsible for the observed nonadiabatic crossing.^{28,30} As we understand more about the nature of the crossing, further calculations on this system will hopefully improve the agreement between theory and experiment and enrich our theoretical picture of the chlorine bond and how it is broken by the absorption of UV light.

In our twisted tale we have recounted so far the stories of two lowly diatomic molecules. We hope we have shown that measurements of a photofragment’s angular momentum can provide us with a new viewpoint for seeing and understanding the process whereby molecules fall apart

under irradiation—a process that is more complicated than might be imagined at first. Our story for each molecule has focused on the complex details of simple systems. Although the study of larger polyatomic molecules brings new and varied challenges, there are many more tales to be followed and games of molecular tennis to be watched with increasingly complex systems.^{21,31–33}

But molecular tennis need not be only a spectator sport. Practicing our molecular wicked cuts, we might explore the ability to control topspins and backspins by the choice of photolysis wavelength and polarization. Indeed, we realize that our game of molecular tennis, regarded in this manner, is really a form of coherent control of a unimolecular decomposition process, a topic that has already captured the imagination of many chemists. Coherent control is based upon the manipulation of which path among equivalent paths connecting initial and final states is followed.^{34,35} We have shown a simple example in which the setting of the phase between two different pathways controls the outcome. In just such a way, we might imagine inducing bonds to follow particular pathways leading to particular products—helping them to break their chains of bondage. Whether such studies will lead to practical consequences or not, they deeply enrich our fundamental understanding of the dynamics of chemical transformations.

We thank Zee Hwan Kim for a critical reading of the manuscript. Support from the NSF (CHE-99-00305) is gratefully acknowledged.

References

- Herzberg, G. *Molecular spectra and molecular structure: Spectra of diatomic molecules*, 2nd ed.; Krieger: Malabar, FL, 1989; Vol. 1.
- Hollas, J. M. *High-resolution spectroscopy*, 2nd ed.; J. Wiley: New York, 1998.
- Wigner, E.; Witmer, E. E. Über die struktur der zweiatomigen molekelspektren nach der quantenmechanik. *Z. Phys.* **1928**, *51*, 859.
- Zare, R. N. *Angular momentum: understanding spatial aspects in chemistry and physics*; Wiley: New York, 1988.
- Atkins, P. W. *Physical chemistry*, 6th ed.; Freeman: New York, 1999.
- McQuarrie, D. A.; Simon, J. D. *Physical chemistry: a molecular approach*; University Science Books: Sausalito, CA, 1997.
- Schinke, R. *Photodissociation dynamics: spectroscopy and fragmentation of small polyatomic molecules*; Cambridge University Press: New York, 1995.
- Murrell, J. N.; Bosanac, S. D. *Introduction to the theory of atomic and molecular collisions*; J. Wiley: New York, 1989.
- Alexander, A. J.; Zare, R. N. Anatomy of elementary chemical reactions. *J. Chem. Educ.* **1998**, *75*, 1105.
- Rakitzis, T. P.; Kandel, S. A.; Alexander, A. J.; Kim, Z. H.; Zare, R. N. Photofragment helicity caused by matter-wave interference from multiple dissociative states. *Science* **1998**, *281*, 1346.
- Ashfold, M. N. R.; Baggott, J. E. *Molecular photodissociation dynamics*; Royal Society of Chemistry: London, 1987.
- Zare, R. N.; Herschbach, D. R. Doppler line shape of atomic fluorescence excited by molecular photodissociation. *Proc. IEEE* **1963**, *51*, 173–182.
- Rakitzis, T. P.; Kandel, S. A.; Alexander, A. J.; Kim, Z. H.; Zare, R. N. Measurement of Cl-atom photofragment angular momentum distributions in the photodissociation of Cl₂ and ICl. *J. Chem. Phys.* **1999**, *110*, 3351.
- Zare, R. N. General discussion. *Faraday Discuss.* **1999**, *113*, 79.
- Simons, J. P. Dynamic stereochemistry and the polarization of reaction products. *J. Phys. Chem.* **1987**, *91*, 5378.
- Hall, G. E.; Houston, P. L. Vector correlations in photodissociation dynamics. *Annu. Rev. Phys. Chem.* **1989**, *40*, 375.
- Dixon, R. N. The determination of the vector correlation between photofragment rotational and translational motions from the analysis of doppler-broadened spectral line-profiles. *J. Chem. Phys.* **1986**, *85*, 1866.
- Brunt, R. J. v.; Zare, R. N. Polarization of atomic fluorescence excited by molecular dissociation. *J. Chem. Phys.* **1968**, *48*, 4304.
- Kupriyanov, D. V.; Vasyutinskii, O. S. Orientation and alignment of ²P_{3/2} fragments following photodissociation of heteroatomic molecules. *Chem. Phys.* **1993**, *171*, 25.
- Eppink, A. T. J. B.; Parker, D. H.; Janssen, M. H. M.; Buijsse, B.; van der Zande, W. J. Production of maximally aligned O(¹D) atoms from two-step photodissociation of molecular oxygen. *J. Chem. Phys.* **1998**, *108*, 1305.
- Ahmed, M.; Peterka, D. S.; Bracker, A. S.; Vasyutinskii, O. S.; Suits, A. G. Coherence in polyatomic photodissociation: aligned O(³P) from photodissociation of NO₂ at 212.8 nm. *J. Chem. Phys.* **1999**, *110*, 4115.
- Rakitzis, T. P.; Zare, R. N. Photofragment angular momentum distributions in the molecular frame: determination and interpretation. *J. Chem. Phys.* **1999**, *110*, 3341.
- Hoffmann, R. A really moving story. *Am. Sci.* **1999**, *87*, 21.
- Siebbeles, L. D. A.; Glass-Maujean, M.; Vasyutinskii, O. S.; Beswick, J. A.; Roncero, O. Vector properties in photodissociation: quantum treatment of the correlation between spatial anisotropy and the angular momentum polarization of the fragments. *J. Chem. Phys.* **1994**, *100*, 3610.
- Zuo, J. M.; Kim, M.; O'Keeffe, M.; Spence, J. C. H. Direct observation of d-orbital holes and Cu–Cu bonding in Cu₂O. *Nature* **1999**, *401*, 49.
- Matsumi, Y.; Tonokura, K.; Kawasaki, M. Fine structure branching ratios and doppler profiles of Cl(²P_{1/2}) photofragments from the photodissociation of the chlorine molecule near and in the ultraviolet. *J. Chem. Phys.* **1992**, *97*, 1065.
- Samartzis, P. C.; Bakker, B. L. G.; Parker, D. H.; Kitsopoulos, T. N. Spin–orbit branching ratios for the Cl-atom photofragments following the excitation of Cl₂ from 310 to 470 nm. *J. Chem. Phys.* **1999**, *110*, 5201.
- Cooper, M. J.; Wrede, E.; Orr-Ewing, A. J.; Ashfold, M. N. R. Ion imaging studies of the Br(²P_{1/2}) atomic products resulting from Br₂ photolysis in the wavelength range 260–580 nm. *J. Chem. Soc., Faraday Trans.* **1998**, *94*, 2901.
- Kim, Z. H.; Alexander, A. J.; Kandel, S. A.; Rakitzis, T. P.; Zare, R. N. Orientation as a probe of photodissociation dynamics; *Faraday Discuss.* **1999**, *113*, 27.
- Alexander, A. J.; Zare, R. N.; Yabushita, S.; Kim, Z. H. General discussion. *Faraday Discuss.* **1999**, *113*, 83.
- Hasselbrink, E.; Waldeck, J. R.; Zare, R. N. Orientation of the CN(X²Σ⁺) fragment following photolysis of ICN by circularly polarized light. *Chem. Phys.* **1988**, *126*, 191.
- Rakitzis, T. P.; Samartzis, P. C.; Kitsopoulos, T. N. Observing the symmetry breaking in the angular distributions of oriented photofragments using velocity mapping. *J. Chem. Phys.* **1999**, *111*, 10415.
- Kim, Z. H.; Alexander, A. J.; Zare, R. N. Speed dependent photofragment orientation in the photodissociation of OCS at 223 nm. *J. Phys. Chem. (Kent Wilson special issue)* **1999**, *103*, 10144.
- Gordon, R. J.; Rice, S. A. Active control of the dynamics of atoms and molecules. *Annu. Rev. Phys. Chem.* **1997**, *48*, 601.
- Shapiro, M.; Brumer, P. Quantum control of chemical reactions. *J. Chem. Soc., Faraday Trans.* **1997**, *93*, 1263.

AR970297E